





## RESEARCH ARTICLE

View Article Online  
View Journal | View IssueCite this: *Inorg. Chem. Front.*, 2021, **8**, 5195

# Gating the photoactivity of azobenzene-type ligands trapped within a dynamic system of an $M_4L_6$ tetrahedral cage, an $M_2L_2$ metallocycle and mononuclear $ML_n$ complexes†

Piotr Cecot, <sup>‡a,b</sup> Anna Walczak, <sup>‡a,b</sup> Grzegorz Markiewicz <sup>b</sup> and Artur R. Stefankiewicz <sup>\*a,b</sup>

Complexation of transition metal ions by a doubly chelating bis(diimine)-type ligand incorporating a photoresponsive azobenzene linker yielded two types of structurally distinct metallocyclic architectures, an  $[M_4L_6]^{8+}$  tetrahedral cage and an  $[M_2L_2]^{4+}$  metallocycle. In solution, these complexes are open for reversible interconversions between each other by varying the  $M:L$  ratio, or switching into a dynamic library of  $[M(L'/L'')]^{2+}$  mononuclear species upon addition of a competing monoamine. While the unbound ligand presents the reversible photoactivity of the azo bond, its complexes are photochemically inert, due to the inherent topology of these assemblies resulting from the restrictions of coordinate bond formation.

Received 20th August 2021,  
Accepted 20th October 2021

DOI: 10.1039/d1qi01063h

rsc.li/frontiers-inorganic

## Introduction

Multistimuli-induced reversibility of chemical bonds is a key challenge of modern chemistry.<sup>1–5</sup> When achieved, one can gain control over the global topology, physicochemical properties and ultimately potential functions of dynamic assembly, for instance, in catalysis to prevent product inhibition or in medicine to release an active compound at a specific site. Structural switching can be achieved by changing the proportion of the added reagents *e.g.* metal ions and/or *via* external stimuli, *e.g.* temperature or light.<sup>6–9</sup> The controlled modulation of more than two dynamic bonds (molecular and/or supramolecular) within a single system remains challenging and is limited to only a few examples.<sup>10–14</sup> Azobenzene derivatives are a well-known class of photoactive compounds that can undergo reversible isomerization upon light irradiation and/or thermal activation. This property has been used for the creation of many advanced photoswitchable systems.<sup>15</sup> The structural and topological control can as well be achieved through component exchange and/or metal-ion coordination, and one of

the most useful units for this is the 2-pyridine-imine *N,N*-chelating center. It owes its popularity to the reversibility of coordinate and imine bonds<sup>16</sup> as well as the convenient synthesis of highly complex metallocyclic structures.<sup>17–19</sup>

Several principles for designing appropriate ligands for multi-walled coordination cages were proposed by, *inter alia*, the Raymond,<sup>20</sup> Fujita, Ballester, Stang, Clever and Nitschke groups.<sup>21–24</sup> The structure of these complexes is subject to the influence of several factors, including ligand shape, host–guest interactions, external environment, and the metal-ion:ligand ratio.<sup>25–31</sup> Thus, depending on the degree of freedom of rotation around the bonds and their stability, one can completely change the structures or adjust their topology to adapt to the guest molecule or other environmental stimuli.

In earlier work, we presented a photochemical study of acyclic azobenzene-substituted metal ion complexes.<sup>32</sup> Although the coordination indeed affected the *trans* → *cis* conversions, the complexes obtained retained the partial photoactivity of the azo bonds, since these were present in unconstrained arms of the ligands. Recently,<sup>33</sup> the retention of photosensitivity was also shown for a  $Pd_2L_4$  type complex based on a bis(pyridylazo)terphenyl ligand. Gated photochromism is much less common but can be achieved in several ways,<sup>34,35</sup> including, *inter alia*, the complexation process. Yamamura *et al.* found that the formation of both macromonocyclic and macrobicyclic complexes of B(III) and Ti(IV), respectively, with catecholate co-ligands led to a complete loss of photosensitivity and locking of the ligand azo unit in its *trans* configuration. The opposite case was found with terpyridine units in place of cate-

<sup>a</sup>Faculty of Chemistry, Adam Mickiewicz University, ul. Uniwersytetu Poznańskiego 8, 61-614 Poznań, Poland. E-mail: ars@amu.edu.pl

<sup>b</sup>Center for Advanced Technologies, Adam Mickiewicz University, Poznań, ul. Uniwersytetu Poznańskiego 10, 61-614 Poznań, Poland

†Electronic supplementary information (ESI) available. CCDC 2060413–2060414. For ESI and crystallographic data in CIF or other electronic format see DOI: 10.1039/d1qi01063h

‡These authors contributed equally in this work.



cholates, where the *cis* form of the ligand was locked in the mononuclear Fe(II) complex.<sup>36,37</sup> To the best of our knowledge no dynamic photochromic system, in which the photosensitivity of the azo bond can be locked by coordination within an  $M_2L_2$  metallocycle, an  $M_4L_6$  tetrahedral cage and a library of  $ML_2/ML_3$  complexes, has been reported.

Herein, we describe the dynamic system of structurally distinct metallosupramolecular assemblies of acyclic and cyclic topologies formed between transition metal ions ( $Zn^{2+}$ ,  $Fe^{2+}$ , and  $Cd^{2+}$ ) and mono- and doubly-chelating azobenzene ligands. In solution, these species are labile, allowing reversible switching between them driven by the changes of the  $M:L$  ratio and/or *via* transimination of the ligands upon addition of competitive amines. While the ligand itself exhibits the typical photochemical activity of azobenzene units, its complexes present gated photochromism upon irradiation, due to the coordination driven locking of the azo bonds within the rigid metallosupramolecular structures.

## Results and discussion

### Synthesis

Ligand *trans*-L was synthesized by the condensation of commercially available pyridine-2-carbaldehyde and *trans*-4,4'-diaminoazobenzene, following a previously reported procedure (Scheme 1, see the ESI† for details).<sup>32</sup> As expected, the ligand was isolated in its thermodynamically favoured pure *trans*-azo form, as confirmed by <sup>1</sup>H NMR spectroscopy (*vide infra*). To a suspension of *trans*-L in acetonitrile, solutions of  $Zn^{2+}$ ,  $Cd^{2+}$  or  $Fe^{2+}$  salts were added, yielding two structurally different complexes, depending on the metal:ligand ratio.  $[M_4L_6]^{8+}$  tetrahedral cages were obtained when *trans*-L was mixed with  $Zn^{2+}$  and  $Fe^{2+}$  salts in a 2 : 3 ratio, while a 1 : 1 ratio yielded  $[M_2L_2]^{4+}$

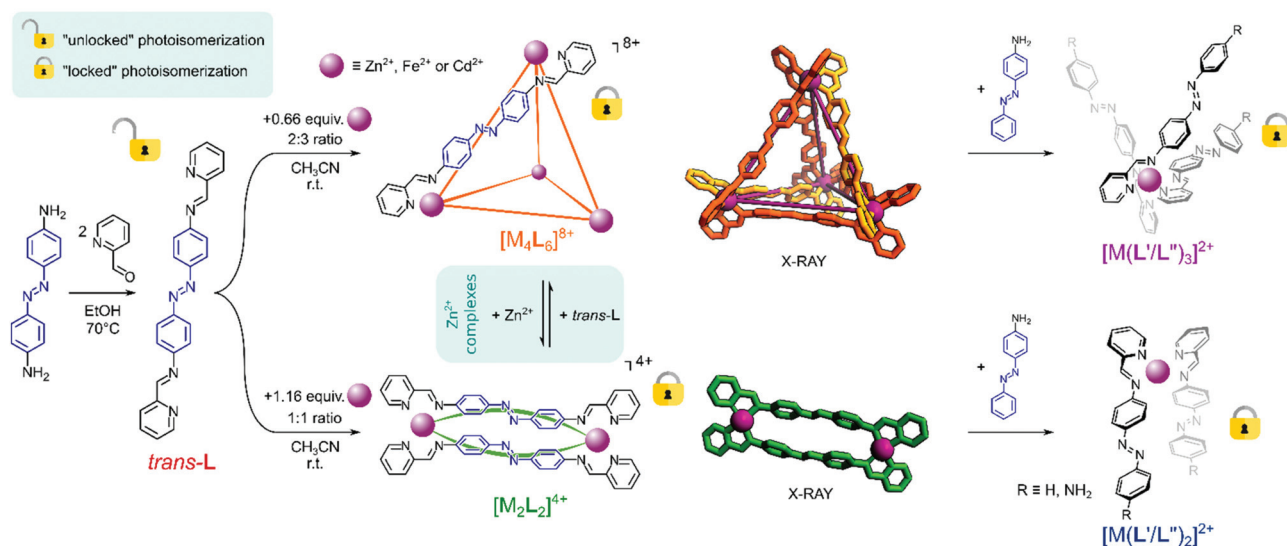
metallocycles for  $Zn^{2+}$  and  $Cd^{2+}$  salts (Scheme 1, see the ESI† for details).

### Solid state study

Slow vapor diffusion of  $Et_2O$  into an acetonitrile solution of  $[Zn_4L_6](ClO_4)_8$  yielded orange crystals, which were characterized by single-crystal X-ray diffraction. The structural determination showed that it crystallizes in the tetragonal space group  $P4_2/n$  with the cation as the  $S_4$  isomer ( $\Delta\Delta\Delta\Delta$  or  $\Lambda\Lambda\Delta\Delta$ ), composed of four equivalent  $Zn^{2+}$  cations coordinated by six *trans*-L molecules (Scheme 1 and Fig. S26a†). Unfortunately, the crystals diffracted weakly, especially in high-angle regions; therefore, the structure was optimized using DFT b3lyp/6-31g (d) computation to locate the missing electron densities (Fig. S26b, see the ESI† for optimization details). The same crystallization technique with the material obtained from the reaction in a 1 : 1 stoichiometry yielded single crystals of the metallocycle  $[Cd_2L_2](ClO_4)_4$  (Fig. S26c†). The complex crystallizes in the triclinic space group  $P\bar{1}$ . Each of the two Cd(II) centres is coordinated by two pyridine-imine units and two  $ClO_4^-$  counterions, which complement both the coordination sphere and the charge of the central  $Cd^{2+}$  cation.

### Solution study

After characterization in the solid state, we focused our studies on solutions to establish the stability of the complexes obtained and to perform photochemical measurements. The <sup>1</sup>H NMR spectra of the ligand *trans*-L,  $[Zn_4L_6](NTf_2)_8$ , and  $[Zn_2L_2](NTf_2)_4$  are shown in Fig. 1. In solution, the ligand exists exclusively as the *trans*-azo isomer, as evidenced by a single set of resonances, with the most indicative being the single imine proton resonance at 8.67 ppm (ref. 38) (*cis*-L form was found upon photoisomerization – *vide infra*). The ligand



**Scheme 1** a) Synthesis of *trans*-L and its  $[M_4L_6](anion)_8$  and  $[M_2L_2](anion)_4$  complexes, followed by reversible interconversion between  $[M_4L_6]^{8+}$  and  $[M_2L_2]^{4+}$  complexes and their switching into a dynamic library of mononuclear  $[M(L'/L'')]_n^{2+}$  species upon transimination of the ligand *trans*-L with 4-aminoazobenzene. Counterions are omitted for clarity; transimination schemes for a (b) tetrahedral cage and (c) metallocycle.



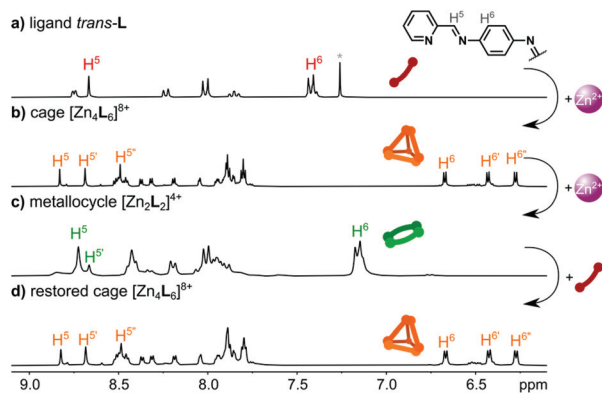


**Fig. 1**  $^1\text{H}$  NMR spectra of (a) ligand *trans*-L (300 MHz,  $\text{CDCl}_3$ ); (b)  $[\text{Zn}_4\text{L}_6](\text{NTf}_2)_8$  cage (300 MHz,  $\text{CD}_3\text{CN}$ ); and (c)  $[\text{Zn}_2\text{L}_2](\text{NTf}_2)_4$  metallocycle (300 MHz,  $\text{CD}_3\text{CN}$ ). (d) Interconversion of  $[\text{Zn}_2\text{L}_2](\text{NTf}_2)_4$  into  $[\text{Zn}_4\text{L}_6](\text{NTf}_2)_8$  upon addition of 0.5 equiv. of *trans*-L.

*trans*-L is non-planar when coordinated and has axial chirality, so its incorporation within the tetrahedral cage structure, along with the four chiral coordination centres (each one with octahedral geometry) could yield a set of diastereoisomeric cages. Considering only the four metal ion centres, three isomers of the  $[\text{M}_4\text{L}_6]^{8+}$  cation are possible:  $S_4$  ( $\Delta\Delta\Delta\Delta$  or  $\Lambda\Lambda\Lambda\Lambda$ ),  $C_3$  ( $\Delta\Delta\Delta\Lambda$  or  $\Lambda\Lambda\Lambda\Delta$ ) and  $T$  ( $\Delta\Delta\Delta\Delta$  or  $\Lambda\Lambda\Lambda\Lambda$ ),<sup>20,25</sup> but, as described above, the species found in the crystal is the pure  $S_4$  isomer, where the chirality of the ligand units appears to be determined by the nature of the metal ion centres that are bridged, so that there are no complications in the stereochemistry arising from this factor.

This is consistent with the fact that the solution  $^1\text{H}$  NMR spectrum of the cage (Fig. 1b) can be resolved into sets of peaks of the  $S_4$ ,  $C_3$  and  $T$  isomers. The  $[\text{Zn}_4\text{L}_6]^{8+}$  cage in acetonitrile solution exists predominantly as the  $S_4$  isomer, as proven by the splitting of the  $\text{H}^5$  imine signals into three well-defined singlets, and splitting and shielding of the  $\text{H}^6$  phenylene signal into three doublets. The molar ratio of the  $S_4$ : $C_3$ : $T$  isomers in acetonitrile solution was found to be 77:20:3 (Fig. S17 and Table S1†), showing that the  $S_4$  form is the favoured isomer of  $[\text{Zn}_4\text{L}_6]^{8+}$  both in solution and the solid state. This isomeric ratio is not affected by the counterion used ( $\text{ClO}_4^-$ ,  $\text{BF}_4^-$ ,  $\text{OTf}^-$ ,  $\text{NTf}_2^-$ ) (Table S1 and Fig. S18, see the ESI† for details). ESI-TOF-MS analysis performed for the cage complex revealed a peak centred at 1103.4846  $m/z$ , assigned to the  $\{[\text{Fe}_4\text{L}_6](\text{OTf})_5\}^{3+}$  ion, a tetranuclear species with the stoichiometry expected for tetrahedral cage-type structures of  $[\text{M}_4\text{L}_6](\text{anion})_8$  complexes (Fig. S11†).

The formation of the cage  $[\text{Zn}_4\text{L}_6]^{8+}$  and the metallocycle  $[\text{Zn}_2\text{L}_2]^{4+}$  was further supported by diffusion ordered NMR spectroscopy (Fig. S7, S15 and Table S3†), which showed the formation of discrete products with diffusion coefficients of  $D = 4.76 \times 10^{-6} \text{ cm}^2 \text{ s}^{-1}$  ( $r = 13.4 \text{ \AA}$ ) and  $D = 5.50 \times 10^{-6} \text{ cm}^2 \text{ s}^{-1}$  ( $r = 11.6 \text{ \AA}$ ), respectively. These radii correspond well to the sizes of the  $[\text{Zn}_4\text{L}_6]^{8+}$  and  $[\text{Zn}_2\text{L}_2]^{4+}$  ions found in the crystal lattices (Fig. S35†).

## Topological switching

To determine whether the interconversion between  $[\text{Zn}_2\text{L}_2]^{4+}$  and  $[\text{Zn}_4\text{L}_6]^{8+}$  is possible, a suspension of *trans*-L in  $\text{CD}_3\text{CN}$  was titrated with  $\text{Zn}(\text{NTf}_2)_2$ . As shown in Fig. S20,† a gradual increase in the  $\text{Zn}^{2+}$  concentration up to a 2:3 M:L ratio led to the exclusive formation of the  $[\text{Zn}_4\text{L}_6]^{8+}$  complex. However, when the M:L ratio exceeded 2:3, the cage began to convert into the  $[\text{Zn}_2\text{L}_2]^{4+}$  metallocycle, yielding at first the cage: metallocycle mixture, then pure  $[\text{Zn}_2\text{L}_2]^{4+}$  after the addition of excess  $\text{Zn}^{2+}$  (Fig. 1c). Finally, the solution of metallocycle  $[\text{Zn}_2\text{L}_2](\text{NTf}_2)_4$  was treated with a suspension of *trans*-L, to observe the direct return of  $[\text{Zn}_2\text{L}_2]^{4+}$  into the  $[\text{Zn}_4\text{L}_6]^{8+}$  species. As shown in Fig. 1d,  $[\text{Zn}_2\text{L}_2]^{4+}$  fully converted into  $[\text{Zn}_4\text{L}_6]^{8+}$  after the addition of 0.5 equiv. of *trans*-L. The subsequent addition of 0.5 equiv. of  $\text{Zn}(\text{NTf}_2)_2$  led to the restoration of the  $[\text{Zn}_2\text{L}_2]^{4+}$  structure (Fig. S21†).

These experiments showed that the complexation of *trans*-L is a dynamic process with an outcome that is directly related to the M:L stoichiometry. The observed interconversions are governed by the relatively strong chelation of  $\text{Zn}(\text{II})$  by the *N,N* donor sites of the ligand, the  $[\text{Zn}_2\text{L}_2]^{4+}$  metallocycle being the least entropically disfavoured species where both  $\text{Zn}(\text{II})$  centres are bis(chelated), and  $[\text{Zn}_4\text{L}_6]^{8+}$  the smallest species where all the  $\text{Zn}(\text{II})$  centres are tris(chelated). The lability of  $\text{Zn}(\text{II})$  means that a variation in the composition of the reaction mixture can be used to enable the isolation of each one of the complexes obtained. In the gas phase, the availability of two coordination sites not occupied by a chelate unit in the metallocyclic complex appears to favour its fragmentation, explaining why multiple attempts to observe  $[\text{M}_2\text{L}_2]^{4+}$  species or their solvates using the ESI-MS technique have failed (see the ESI† for details).

## Photoactivity

The photochemical behaviour of *trans*-L and the complexes  $[\text{Zn}_4\text{L}_6](\text{NTf}_2)_8$  and  $[\text{Zn}_2\text{L}_2](\text{NTf}_2)_4$  was investigated by electronic absorption and  $^1\text{H}$  NMR spectroscopy (Fig. 2). The ligand *trans*-L shows behaviour typical of azobenzene derivatives that undergo reversible *trans*  $\rightarrow$  *cis* photoisomerization of the azo bond induced by UV light. Irradiation of *trans*-L solutions in acetonitrile (UV-vis) or chloroform (NMR) with near-UV light ( $\lambda_{\text{max}} = 395 \text{ nm}$ ) results in its partial isomerization to *cis*-L, as indicated by a gradual decrease in the absorption intensity of the  $\pi \rightarrow \pi^*$  azo band ( $\lambda_{\text{max}} = 380 \text{ nm}$ ) in the absorption spectrum (Fig. S27a†), and appearance of a new set of shielded resonances in the  $^1\text{H}$  NMR spectrum (Fig. 2a). Plotting those changes as a function of irradiation time revealed that the reaction follows reversible first-order kinetics, with a ( $k = k_{\text{trans} \rightarrow \text{cis}} + k_{\text{cis} \rightarrow \text{trans}}$ ) rate constant of  $0.74 \text{ s}^{-1}$  (Fig. S27b†). The reaction equilibrates at 62% of *cis*-L in the photostationary state ( $K = 1.63$ ) with isomerization rate constants of  $k_{\text{trans} \rightarrow \text{cis}} = 0.46 \text{ s}^{-1}$  and  $k_{\text{cis} \rightarrow \text{trans}} = 0.28 \text{ s}^{-1}$ .

Upon heating the *cis/trans*-L mixture converts back from PSS to a pure *trans*-L isomer. The thermally driven reaction clearly follows first-order kinetics with  $k'_{\text{cis} \rightarrow \text{trans}} \text{ thermal} = 2.4$



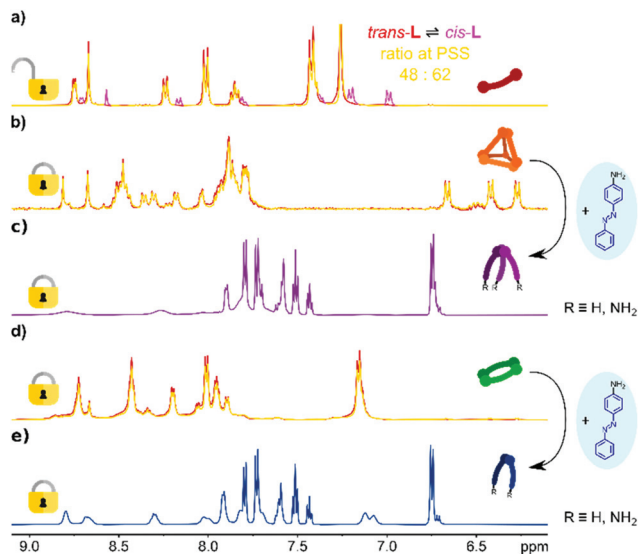


**Fig. 2**  $^1\text{H}$  NMR spectra (600 MHz) of (a) ligand *trans*-L in  $\text{CDCl}_3$  before (red) and after irradiation (yellow); signals of *cis*-L marked in magenta. (b)  $[\text{Zn}_4\text{L}_6](\text{NTf}_2)_8$  cage in  $\text{CD}_3\text{CN}$  before (red) and after irradiation (yellow). (c) Conversion of the  $[\text{Zn}_4\text{L}_6](\text{NTf}_2)_8$  cage in  $\text{CD}_3\text{CN}$  into a library of  $[\text{M}(\text{L}'/\text{L}'')_3]^{2+}$  species after addition of 4-aminoazobenzene (for full titration spectra, see Fig. S22†). (d)  $[\text{Zn}_2\text{L}_2](\text{NTf}_2)_4$  metallocycle in  $\text{CD}_3\text{CN}$  before (red) and after irradiation (yellow). (e) Conversion of the  $[\text{Zn}_2\text{L}_2](\text{NTf}_2)_4$  metallocycle in  $\text{CD}_3\text{CN}$  into a library of  $[\text{M}(\text{L}'/\text{L}'')_2]^{2+}$  species after addition of 4-aminoazobenzene (for full titration spectra, see Fig. S23 and S24†).

$10^{-3} \text{ s}^{-1}$  and  $t_{1/2} = 288 \text{ s}$  at 333 K (Fig. S34a and 34b†). Both photochemical and thermal reactions were found to be fully reversible in irradiation/heating cycles (Fig. S30 and S31†).

In contrast to our previous study,<sup>32</sup> where the photoactive moieties were placed in the outer coordination sphere, the azobenzene units of both the  $[\text{M}_4\text{L}_6]^{8+}$  cage and the  $[\text{M}_2\text{L}_2]^{4+}$  metallocycle are tied up within the cyclic and rigid coordination structures. Taking into account that the *trans*  $\rightarrow$  *cis* isomerization of the azo bond leads to a significant shortening of the L molecule, and a subsequent change in the angle between two chelating centres, photoisomerization of the bound ligand in the complexes would be expected to lead to rearrangement into species of quite different topology. Indeed, in the past irradiation has been shown to lead to complete dissociation of a metallocage species derived from a ligand incorporating two diazo units linking simple pyridine donors.<sup>33</sup>

The absorption spectra of both  $[\text{Zn}_4\text{L}_6](\text{NTf}_2)_8$  and  $[\text{Zn}_2\text{L}_2](\text{NTf}_2)_4$  show similar profiles to that of the *trans*-L spectrum, with  $\lambda_{\text{max}}$  values at 362 and 372 nm, respectively. Irradiation of their solutions under identical conditions to those found to isomerize *trans*-L, gave, however, unexpected results. Namely, both cage and metallocycle showed high resistance to photoisomerization, yielding only <10% conversions in the photo-stationary state achieved after prolonged photoirradiation (Fig. S28 and S29†). Given that the measurements were made on very dilute solutions (required for absorption spectroscopy), and the formation of both  $[\text{Zn}_4\text{L}_6]^{8+}$  and  $[\text{Zn}_2\text{L}_2]^{4+}$  complexes is

reversible, it was concluded that the observed conversions most likely originated from the released *trans*-L molecules, not from the complexes. Indeed, when the irradiated samples of  $[\text{Zn}_4\text{L}_6]^{8+}$  and  $[\text{Zn}_2\text{L}_2]^{4+}$  were heated to induce a backward *cis*  $\rightarrow$  *trans* conversion, an abnormal release of *trans*-L was observed. In contrast to the isolated L, the first-order backward isomerisation is affected by the disassembly processes so the conversion exceeds 100% of *trans*-L (Fig. S34c and 34d†).

To omit the problem with the partial disassembly, we followed the isomerization by  $^1\text{H}$  NMR spectroscopy, which allows the use of higher concentrations and observation of all species in the solution. As shown in Fig. 2b, UV irradiation of the  $[\text{Zn}_4\text{L}_6](\text{NTf}_2)_8$  cage does not lead to any observable changes. All resonances remain unchanged, proving that the cage is photochemically stable, in terms of azo bond photoisomerization. Similar results were obtained for  $[\text{Zn}_2\text{L}_2](\text{NTf}_2)_4$  (Fig. 2d), proving that the metallocyclic structure is also photochemically locked. Having the photoactive ligand L, and its photochemically inert complexes, we decided to check if it is possible to introduce the *cis*-L into assemblies prior to the complexation. However, when the mixture of *trans/cis*-L was treated with  $\text{Zn}^{2+}$  salt we observed a gradual decrease in the absorbance, without indicative red/blue shifts for the selective formation of metallosupramolecular assemblies. Coordination also does not stimulate the reverse isomerization of the azo unit, even when the mixture with an excess of a metal salt is allowed to stand for 24 h for a spontaneous *cis*  $\rightarrow$  *trans* backward conversion (Fig. S32†).

### Transimination

Having the photoinactive cyclic complexes, we decided to examine whether they could be converted into acyclic products *via* the transimination reaction and thus possibly modulate the photosensitivity of the azo units. Addition of the competing 4-aminoazobenzene into a solution of  $[\text{Zn}_4\text{L}_6](\text{NTf}_2)_8$  in  $\text{CD}_3\text{CN}$  yielded, through a transimination reaction, a library of mononuclear  $[\text{M}(\text{L}'/\text{L}'')_3]^{2+}$  octahedral complexes bearing azobenzene units (Scheme 1 and Fig. 2c). Similar changes were observed for the  $[\text{Zn}_2\text{L}_2](\text{NTf}_2)_4$  metallocycle, which was also converted into a library of mononuclear complexes, although due to the limited number of ligands formed, the reaction yielded  $[\text{M}(\text{L}'/\text{L}'')_2]^{2+}$  species (Scheme 1 and Fig. 2e). Our previous work<sup>32</sup> has shown that the mononuclear  $[\text{ML}_n]^{i+}$  complexes bearing azobenzene moieties retain some partial photoactivity of the azobenzene unit despite the metal ion complexation. However, when the dynamic libraries of  $[\text{M}(\text{L}'/\text{L}'')_3]^{2+}$  and  $[\text{M}(\text{L}'/\text{L}'')_2]^{2+}$  complexes were subjected to UV radiation, we did not observe a significant increase in their photoactivity (*trans*  $\rightarrow$  *cis* conversions were found to be about 10% for both libraries; Fig. S33†).

## Conclusions

In conclusion, a new dynamic metallosupramolecular system consisting of photoactive ligands and transition metal ions in



which photoactivity can be restricted by topology changes has been obtained. Depending on the M:L ratio, two types of cyclic complexes, *i.e.*  $[M_4L_6]^{8+}$  tetrahedral cages and  $[M_2L_2]^{4+}$  metallocycles, have been generated. We have shown that the self-assembly of both tetrahedral cages and metallocycle species is a dynamic process, allowing reversible interconversion between both structures steered by the M:L ratio. What is more, the transimination reaction observed upon addition of monoamine into  $[M_2L_2]^{4+}$  and  $[M_4L_6]^{8+}$  solutions yielded dynamic libraries of the mononuclear  $[M(L'/L'')_2]^{2+}$  and  $[M(L'/L'')_3]^{2+}$  complexes, respectively. Photochemical studies have shown that while the uncoordinated ligand displays typical behaviour of photoactive azobenzene derivatives, its macrocyclic complexes resist isomerization due to the locking of the azo bonds within the rigid metallocycle topologies.

## Conflicts of interest

There are no conflicts to declare.

## Acknowledgements

A. R. S. and A. W. thank the National Science Centre (grant SONATA BIS 2018/30/E/ST5/00032) for financial support. We thank Prof. J. M. Harrowfield and Prof. J. R. Nitschke for helpful discussions. This work was supported by the INNOCHEM (grant no. POWR.03.02.00-00-I023/17) co-financed by the European Union through the European Social Fund under the Operational Program Knowledge Education Development. The calculations were carried out at the Poznań Supercomputing and Networking Center (grant no. 401). A. W. and G. M. are supported by the Foundation for Polish Science (FNP).

## Notes and references

- J. Hu, S. K. Gupta, J. Ozdemir and M. H. Beyzavi, Applications of Dynamic Covalent Chemistry Concept towards Tailored Covalent Organic Framework Nanomaterials: A Review, *ACS Appl. Nano Mater.*, 2020, **3**, 6239–6269.
- Y. Jin, C. Yu, R. J. Denman and W. Zhang, Recent advances in dynamic covalent chemistry, *Chem. Soc. Rev.*, 2013, **42**, 6634–6654.
- J. R. Nitschke, Supramolecular and dynamic covalent reactivity, *Chem. Soc. Rev.*, 2014, **43**, 1798–1799.
- J. M. Lehn, From supramolecular chemistry towards constitutional dynamic chemistry and adaptive chemistry, *Chem. Soc. Rev.*, 2007, **36**, 151–160.
- S. J. Rowan, S. J. Cantrill, G. R. L. Cousins, J. K. M. Sanders and J. F. Stoddart, Dynamic Covalent Chemistry, *Angew. Chem., Int. Ed.*, 2002, **41**, 898–952.
- M. Schmittel, Dynamic Functional Molecular Systems: From Supramolecular Structures to Multi-Component Machinery and to Molecular Cybernetics, *Isr. J. Chem.*, 2019, **59**, 197–208.
- P. Tecilla and D. Bonifazi, Configurational Selection in Azobenzene-Based Supramolecular Systems Through Dual-Stimuli Processes, *ChemistryOpen*, 2020, **9**, 529–544.
- E. Moulin, L. Faour, C. C. Carmona-Vargas and N. Giuseppone, From Molecular Machines to Stimuli-Responsive Materials, *Adv. Mater.*, 2020, **32**, 1906036.
- R. Gostl, A. Senf and S. Hecht, Remote-controlling chemical reactions by light: towards chemistry with high spatio-temporal resolution, *Chem. Soc. Rev.*, 2014, **43**, 1982–1996.
- H. M. Seifert, K. Ramirez Trejo and E. V. Anslyn, Four Simultaneously Dynamic Covalent Reactions. Experimental Proof of Orthogonality, *J. Am. Chem. Soc.*, 2016, **138**, 10916–10924.
- J. Septavaux, C. Tosi, P. Jame, C. Nervi, R. Gobetto and J. Leclaire, Simultaneous CO<sub>2</sub> capture and metal purification from waste streams using triple-level dynamic combinatorial chemistry, *Nat. Chem.*, 2020, **12**, 202–212.
- S. Lascano, K. D. Zhang, R. Wehlauch, K. Gademann, N. Sakai and S. Matile, The third orthogonal dynamic covalent bond, *Chem. Sci.*, 2016, **7**, 4720–4724.
- L. Rocard, A. Berezin, F. De Leo and D. Bonifazi, Templated Chromophore Assembly by Dynamic Covalent Bonds, *Angew. Chem., Int. Ed.*, 2015, **54**, 15739–15743.
- R. J. Sarma, S. Otto and J. R. Nitschke, Disulfides, imines, and metal coordination within a single system: interplay between three dynamic equilibria, *Chem. – Eur. J.*, 2007, **13**, 9542–9546.
- J. Dokic, M. Gothe, J. Wirth, M. V. Peters, J. Schwarz, S. Hecht and P. Saalfrank, Quantum chemical investigation of thermal cis-to-trans isomerization of azobenzene derivatives: substituent effects, solvent effects, and comparison to experimental data, *J. Phys. Chem. A*, 2009, **113**, 6763–6773.
- M. E. Belowich and J. F. Stoddart, Dynamic imine chemistry, *Chem. Soc. Rev.*, 2012, **41**, 2003–2024.
- D. Zhang, T. K. Ronson and J. R. Nitschke, Functional Capsules via Subcomponent Self-Assembly, *Acc. Chem. Res.*, 2018, **51**, 2423–2436.
- S. Zarra, D. M. Wood, D. A. Roberts and J. R. Nitschke, Molecular containers in complex chemical systems, *Chem. Soc. Rev.*, 2015, **44**, 419–432.
- A. J. McConnell, C. S. Wood, P. P. Neelakandan and J. R. Nitschke, Stimuli-Responsive Metal-Ligand Assemblies, *Chem. Rev.*, 2015, **115**, 7729–7793.
- D. L. Caulder and K. N. Raymond, Supermolecules by Design, *Acc. Chem. Res.*, 1999, **32**, 975–982.
- D. A. Roberts, B. S. Pilgrim and J. R. Nitschke, Covalent post-assembly modification in metallocycle chemistry, *Chem. Soc. Rev.*, 2018, **47**, 626–644.
- R. Chakrabarty, P. S. Mukherjee and P. J. Stang, Supramolecular coordination: self-assembly of finite two- and three-dimensional ensembles, *Chem. Rev.*, 2011, **111**, 6810–6918.



- 23 P. Ballester, M. Fujita and J. Rebek Jr., Molecular containers, *Chem. Soc. Rev.*, 2015, **44**, 392–393.
- 24 M. Han, D. M. Engelhard and G. H. Clever, Self-assembled coordination cages based on banana-shaped ligands, *Chem. Soc. Rev.*, 2014, **43**, 1848–1860.
- 25 W. Meng, J. K. Clegg, J. D. Thoburn and J. R. Nitschke, Controlling the transmission of stereochemical information through space in terphenyl-edged Fe<sub>4</sub>L<sub>6</sub> cages, *J. Am. Chem. Soc.*, 2011, **133**, 13652–13660.
- 26 A. M. Johnson, M. C. Young and R. J. Hooley, Reversible multicomponent self-assembly mediated by bismuth ions, *Dalton Trans.*, 2013, **42**, 8394–8401.
- 27 J. K. Clegg, J. Cremers, A. J. Hogben, B. Breiner, M. M. J. Smulders, J. D. Thoburn and J. R. Nitschke, A stimuli responsive system of self-assembled anion-binding Fe<sub>4</sub>L<sub>6</sub><sup>8+</sup> cages, *Chem. Sci.*, 2013, **4**, 68–76.
- 28 A. M. Johnson, C. A. Wiley, M. C. Young, X. Zhang, Y. Lyon, R. R. Julian and R. J. Hooley, Narcissistic self-sorting in self-assembled cages of rare Earth metals and rigid ligands, *Angew. Chem., Int. Ed.*, 2015, **54**, 5641–5645.
- 29 S. J. Wezenberg, Light-switchable Metal-Organic Cages, *Chem. Lett.*, 2020, **49**, 609–615.
- 30 A. Brzechwa-Chodzyńska, W. Drożdż, J. Harrowfield and A. R. Stefankiewicz, Fluorescent sensors: A bright future for cages, *Coord. Chem. Rev.*, 2021, **434**, 213820.
- 31 R. G. Siddique, K. S. A. Arachchige, H. A. Al-Fayaad, A. J. Brock, A. S. Micallef, E. T. Luis, J. D. Thoburn, J. C. McMurtrie and J. K. Clegg, The kinetics and mechanism of interconversion within a system of [Fe<sub>2</sub>L<sub>3</sub>]<sup>4+</sup> helicates and [Fe<sub>4</sub>L<sub>6</sub>]<sup>8+</sup> cages, *Chem. Commun.*, 2021, **57**, 4918–4921.
- 32 G. Markiewicz, A. Walczak, F. Perlitius, M. Piasecka, J. M. Harrowfield and A. R. Stefankiewicz, Photoswitchable transition metal complexes with azobenzene-functionalized imine-based ligands: structural and kinetic analysis, *Dalton Trans.*, 2018, **47**, 14254–14262.
- 33 S. Fu, Q. Luo, M. Zang, J. Tian, Z. Zhang, M. Zeng, Y. Ji, J. Xu and J. Liu, Light-triggered reversible disassembly of stimuli-responsive coordination metallocupramolecular Pd<sub>2</sub>L<sub>4</sub> cages mediated by azobenzene-containing ligands, *Mater. Chem.*, 2019, **3**, 1238–1243.
- 34 M. Lohse, K. Nowosinski, N. L. Traulsen, A. J. Achazi, L. K. von Krbek, B. Paulus, C. A. Schalley and S. Hecht, Gating the photochromism of an azobenzene by strong host-guest interactions in a divalent pseudo[2]rotaxane, *Chem. Commun.*, 2015, **51**, 9777–9780.
- 35 G. Baggi, L. Casimiro, M. Baroncini, S. Silvi, A. Credi and S. J. Loeb, Threading-gated photochromism in [2]pseudorotaxanes, *Chem. Sci.*, 2019, **10**, 5104–5113.
- 36 M. Yamamura, Y. Okazaki and T. Nabeshima, Photoisomerization locking of azobenzene by formation of a self-assembled macrocycle, *Chem. Commun.*, 2012, **48**, 5724–5726.
- 37 M. Yamamura, K. Yamakawa, Y. Okazaki and T. Nabeshima, Coordination-driven macrocyclization for locking of photo- and thermal *cis*→*trans* isomerization of azobenzene, *Chem. – Eur. J.*, 2014, **20**, 16258–16265.
- 38 Y. Jung, J. Nam, J.-H. Kim and W.-D. Jang, Hydrophilic–hydrophobic phase transition of photoresponsive linear and macrocyclic poly(2-isopropyl-2-oxazoline)s, *RSC Adv.*, 2017, **7**, 10074–10080.

